Testing of high heat flux 3D printed aluminium evaporators

Henk Jan van Gerner[1], Marc de Smit, Derron van Helvoort, and Johannes van Es[2]
National Aerospace Laboratory NLR, Amsterdam, The Netherlands

The amount of waste heat that is generated in electronic components in aerospace application is increasing because of higher electrical power demands. As a result, conventional cooling methods are not able to maintain the electronic component below its maximum temperature. For this reason, a two-phase Mechanically Pumped Fluid Loop is being developed for high-power electronic components in a commercial aerospace application. These electronic components generate a heat load of 722 W on a 3.8 cm x 3.8 cm surface, resulting in a heat flux of 50 W/cm^2. Tests with 8 different evaporator samples were carried out to determine the heat transfer coefficients and pressure drop and to select the optimal evaporator sample that is further developed in the detail design phase of the project. The tests show that the 3D printed aluminium evaporators are able to keep the heat source well below its maximum temperature.

Nomenclature

h	- Heat transfer coefficient (W/(m^{2}K))
h_{lv}	- Specific latent heat of vaporization (J/kg)
k	- Thermal conductivity (W/(mK))
P	- Heat input/output (W)
q	- Heat flux (W/m^2)
s	- Distance between temperature sensor and channel wall (m)
T	- Temperature (°C)
T_{sat}	- Saturation temperature (°C)
x	- Vapour mass fraction (-)
R245fa	- Pentafluoropropane
SLS	- Selective Laser Sintering
TPTF	- Two-Phase Test Facility
2Φ-MPFL	- Two-phase Mechanically Pumped Fluid Loop

I. Introduction

Modern aircraft and spacecraft rely on growing numbers of electronic components onboard, which in turn are increasingly high-powered and compact. Conventional cooling methods have become too large and heavy and have thus become a bottle-neck in aerospace systems. In some instances, they cannot supply the required cooling performances and keep devices below their specified maximum temperatures. For this reason, a two-phase Mechanically Pumped Fluid Loop (2Φ-MPFL) is being developed for high-power electronic components in a commercial aerospace application. As depicted in Figure 1, a pump circulates the fluid (also known as the refrigerant). The fluid flows through an evaporator downstream of the pump, which physically interfaces with the electronic component to be cooled. The heat from the component is conducted towards the circulating fluid, causing it to evaporate. The liquid-vapor mixture then flows to a condenser where it returns to its liquid phase. A recuperator is often applied to warm the cold liquid that comes from the pump by using the waste heat from the liquid/vapor mixture that comes from the evaporator.

The key advantage of a two-phase system over a conventional single-phase system is that the required mass-flow for a 2Φ-MPFL is substantially less for a given heat load, allowing for smaller tubing diameter and component dimensions to be used in its design; As a result, 2Φ-MPFL tend to be both more compact and less heavy than their single-phase counterparts. Furthermore, due to phase change of the fluid (evaporation and condensation) the

[1] R&D Engineer, Space Systems, Henk.Jan.van.Gerner@nlr.nl, +31 88 511 4628.
[2] R&D Manager, Space Systems, Johannes.van.Es@nlr.nl, +31 88 511 4230

temperature of the liquid/vapor mixture is nearly the same in the entire system, and independent of the heat input. This results in an uniform temperature of the electronic component's surface.

The 2Φ-MPFL system considered in this paper uses the refrigerant pentafluoropropane (R245fa) as heat carrier fluid and operates at a saturation temperature of 95°C. As part of the preliminary design phase of the cooling system, tests were carried out on evaporator samples to determine the heat transfer coefficients and pressure drop and to select the evaporator sample that is further developed in the detail design phase. This paper describes these tests on the evaporator samples.

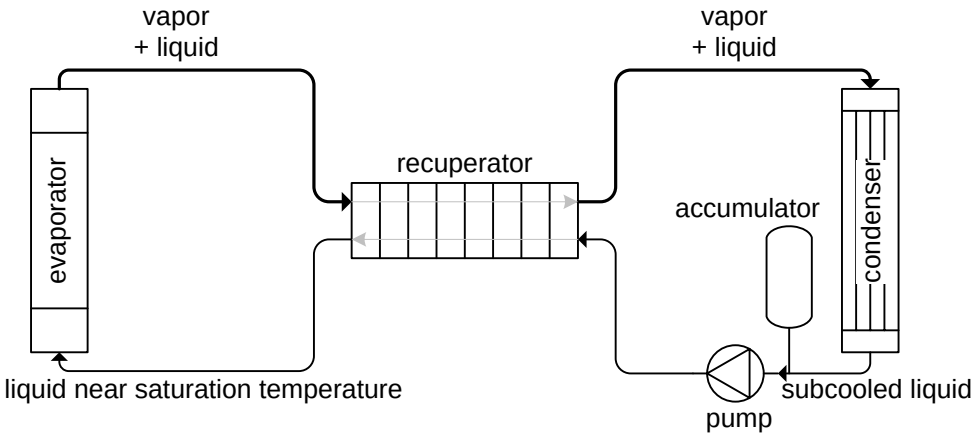

Figure 1 Schematic drawing of a basic 2Φ-MPFL

II. Problem description

In the intended application, there are several electronic components that generate a waste heat of 722 W each on a 3.8 cm x 3.8 cm surface (14.4 cm^2). This results in a heat flux of 50 W/cm^2. The evaporator absorbs the waste heat from these electronic components. The evaporator contains small channels through which fluid is pumped. This fluid is nearly isothermal. However, there can be a large temperature difference between the fluid and the evaporator. This temperature difference can be calculated with the Heat Transfer Coefficient (HTC, see section V). The HTC can vary significantly depending on the fluid, channel diameter, heat flux, mass flux, and vapour mass fraction. When the heat flux is high (e.g. 50 W/cm^2) a phenomenon which is called 'dry-out' can occur. This means that locally the wall of the evaporator is not wetted by liquid anymore, which results in a sudden drop in HTC and too high temperatures. These high temperatures can damage the electronic components and must be prevented. The dry-out phenomenon is illustrated in Figure 2, which shows a drawing of dry-out in an evaporator channel. The liquid core in the channel is surrounded by vapour, which results in a very low HTC. Unfortunately, current empirical evaporation models for heat transfer and dry-out are very inaccurate at the temperature and heat flux that is required in this project. For this reason, tests have been carried out on 8 different evaporator samples. One sample has simple straight parallel channels and acts as a baseline design. The other samples have internal geometries that are aimed to promote mixing of the flow to homogenize the fluid. Sharp corners, sudden expansions and contractions are used in diverse ways in each sample and are presented in more detail in Section III B. Empirical pressure drop correlations were used to aim for a pressure drop of 0.6 bars, the theoretical pressure drops of the baseline sample.

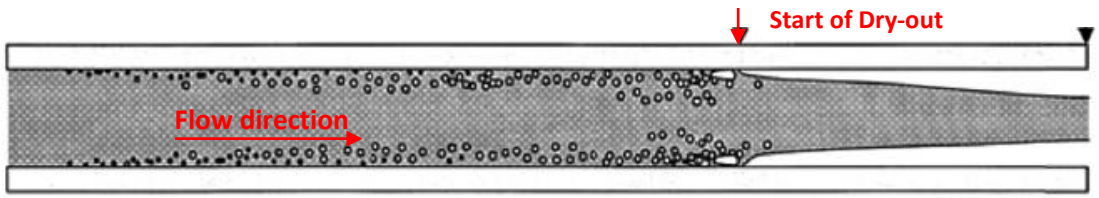

Figure 2 Schematic drawing of dry-out in an evaporator channel[1]

..

III. Evaporator test samples

A. General layout of the samples

Figure 3 and Figure 4 show the general layout of the 8 test samples. The samples are made from 3D printed aluminium (AlSi10Mg) using Selective Laser Sintering[3]. The heated surface is divided into 8 segments by 1 mm deep grooves. Using electric discharge machine drilling, temperature sensor shafts were positioned 1 mm under each segment surface; the temperature sensor shafts have a 0.6 mm diameter and are 12 mm deep. Each segment can be heated using cartridge heaters that are embedded in an adjacent copper block (see Figure 6) with mirrored segmentation and temperature sensor shaft positioning. The temperatures of the evaporator segments and adjacent copper block heater segments can thus be isolated, allowing for the calculation of the HTC of each segment. This allows for the detection of dry-out in the sample (in which case the segment near the outlet will be hotter than the other segments), and for the detection of an unequal flow distribution over parallel channels (in which case the left or right side of the sample will become hotter than the other side). The total heated area of the sections is 14.4 cm^2. The total electrical heat dissipation capacity of the 5 cartridge heaters in the copper block is 722W, which results in a heat flux of 50 W/cm^2 at the test sample interface. At a heat input of 722W, the temperature at the top surface of the copper block is 30°C higher than at the bottom, due to thermal conductance through the copper. Figure 7 shows the labels that are used for the 16 temperature sensors in the evaporator and heater block. Figure 5 shows a photo of two samples just after they came out of the 3D printer. The 8 different samples are discussed in more detail in the next sections.

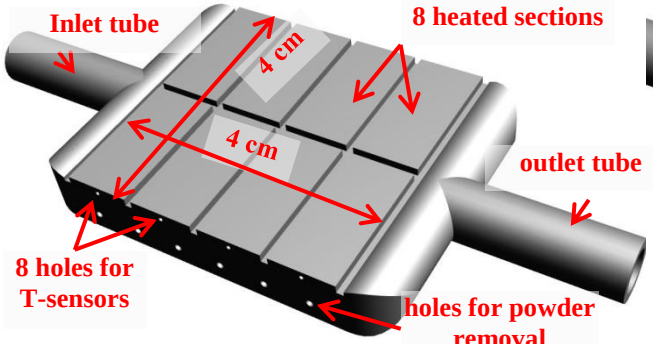

Figure 3 Bottom view of the test sample

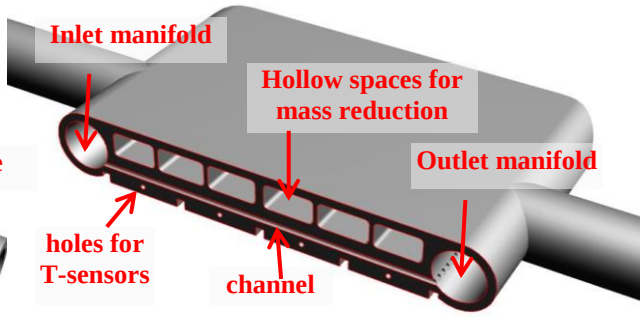

Figure 4 Top view cross-section of the test sample

Figure 5 Photo of some samples as they come out of the 3D printer (so before post-processing)

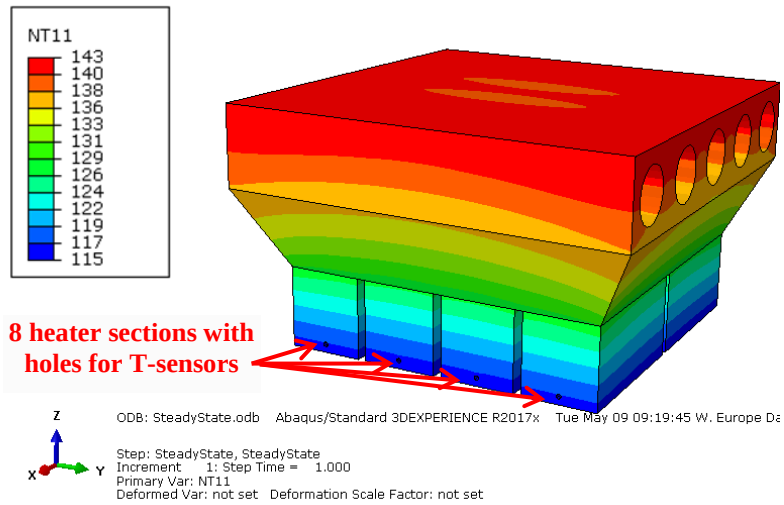

Figure 6 Analysis of the temperature distribution of the copper heater block using a finite element method. The numbers in the box indicate temperatures in °C.

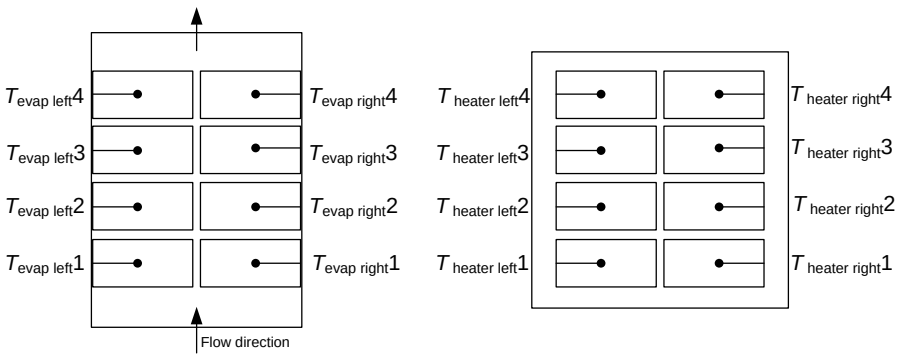

Figure 7 Labels of the 16 temperature sensors in the evaporator and copper heater block

B. Evaporator samples

Eight different evaporator samples were designed, fabricated and tested. The samples were designed for a thermal power input of 722W and a vapour mass fraction at the outlet of 0.2. Each sample was sized for a theoretical pressure drop of approximately 0.6 bar – the expected theoretical pressure drops of the straight channels – but is subject to a large uncertainty. The frictional pressure drop across the sample in each straight segment is modelled using the two-phase Muller-Steinhagen and Heck pressure drop correlation, which is relative accurate[4]. The pressure drop due to sharp bends and sudden channel diameter changes are modelled with the use of empirical minor pressure loss factors[5]. These pressure loss factors are subject to large uncertainties, which makes it difficult to accurately calculate the pressure drop for complex internal channel geometries.

The main sample design parameters are presented in Table 1. Sample 1 is the baseline sample composed of straight parallel channels which is illustrated in Figure 8. Figure 9 shows a cross section of a sample 4 with zigzag channels while Figure 10 shows sample 8 with channel restrictions. Cross sections of the other samples are shown in the Appendix.

Table 1 Description of the different evaporator samples

	Sample name	Number of parallel channels	Channel diameter [mm]	Description
1	Straight-channels	39	0.60	Straight parallel channels (baseline design)
2	Step-diameter-change	23	0.88-1.32	Sudden diameter changes in straight parallel channels
3	Cone-diameter-change	26	0.75-1.12	Ramp changes in diameter of straight parallel channels
4	Zigzag channels	29	0.80	Sharp changes in channel orientation along the flow direction
5	Split-combine-channels	16	0.68-0.96	Periodical splitting and merging of channel from 2x 0.68 to 1x 0.96 mm
6	Liquid injection serial channel	1	3.00 & 4.00	Meandering channel, 81 injections through 0.2mm holes.
7	Liquid injection parallel channels	39	0.60	Parallel meandering channels, 4 injections per channel, 0.2 mm holes.
8	Channel-restrictions	25	0.80-1.20	Periodic constriction and subsequent expansion along parallel channels

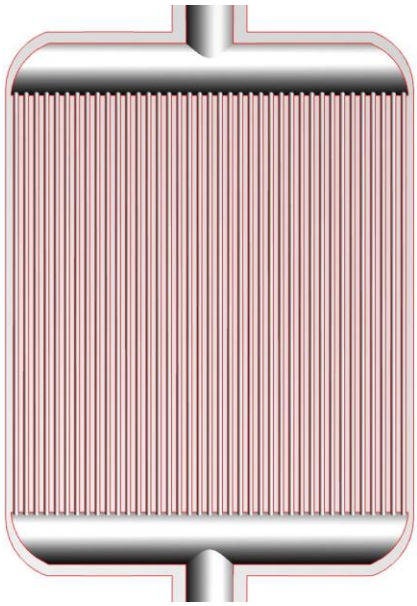

Figure 8 Evaporator sample 1 with straight parallel channels

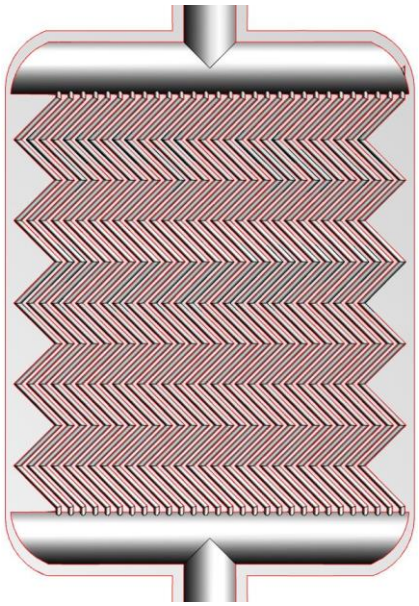

Figure 9 Evaporator sample 4 with 'zigzag' channels

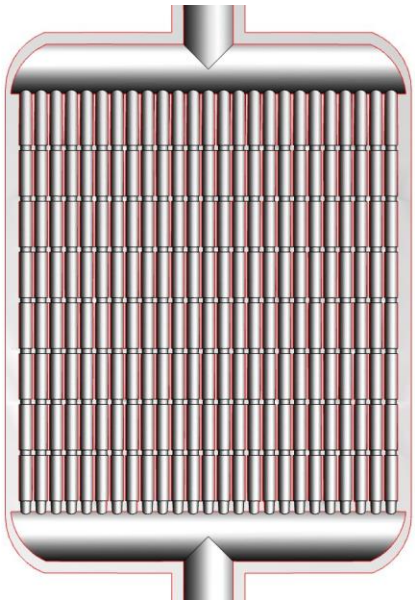

Figure 10 Evaporator sample 8 with channels with restrictions

IV. Test setup

The NLR Two-Phase Test Facility (TPTF) is a two-phase Mechanically Pumped Fluid Loop that has been built by the NLR and is used for component and concept testing. Figure 11 and Figure 12 show photos of the facility with and without insulation. The TPTF is built such that components can easily be replaced and tested, which greatly reduce the development time and costs for new component and systems. A further description of the TPTF is provided in reference[2].

To test the 3D printed evaporator samples, the three standard evaporators in the TPTF are replaced by the 8 aluminium evaporator samples that were discussed in the previous section. Figure 13 shows a schematic drawing of the modified TPTF and Figure 14 shows a photo. All 8 samples are installed in the test setup. Ball valves are used to allow flow through a specific evaporator, while the flow through the other 7 evaporators is blocked. The copper block that is used to apply the heat is attached to one evaporator and insulation is applied around the copper block and evaporator. Figure 15 shows a photo of an evaporator with copper block covered in insulation. Each evaporator can be rotated with 90° to investigate the influence of gravity on the flow distribution over the parallel channels.

Figure 11 Photo of the Test Facility without insulation

Figure 12 Photo of the Test Facility with insulation

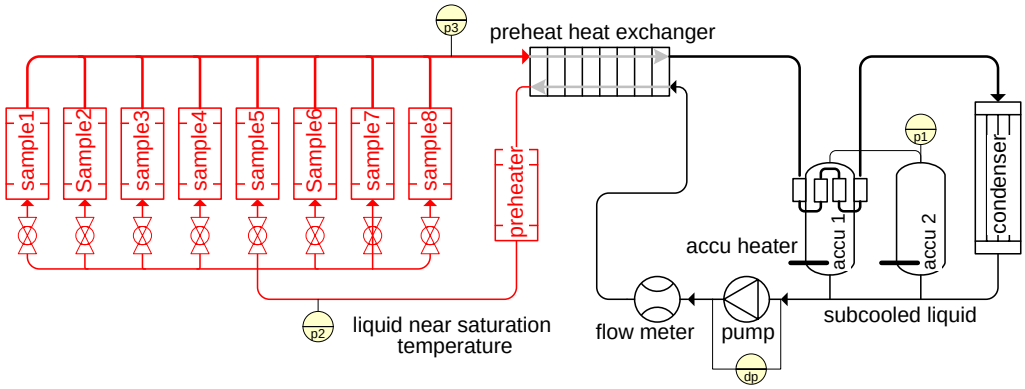

Figure 13 Schematic drawing of the modified Two-Phase Test Facility. The modifications are indicated in red

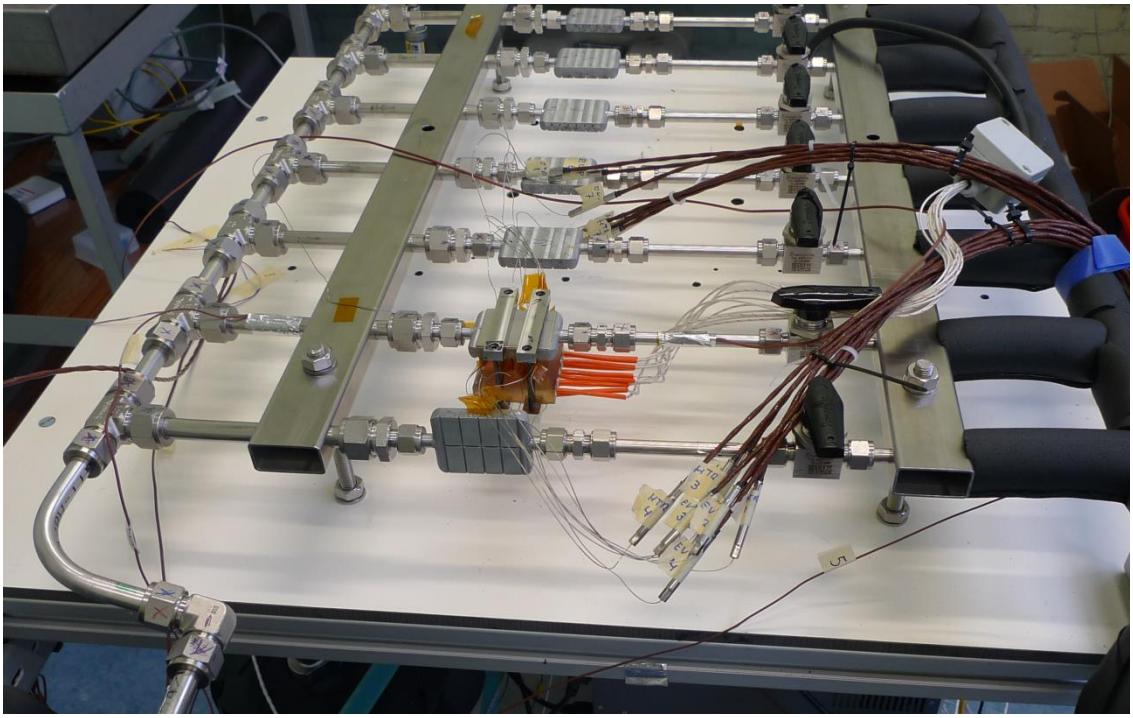

Figure 14 Photo of the modified setup with the 8 evaporators installed. Note that in this photo, evaporator 1 is rotated with 90°

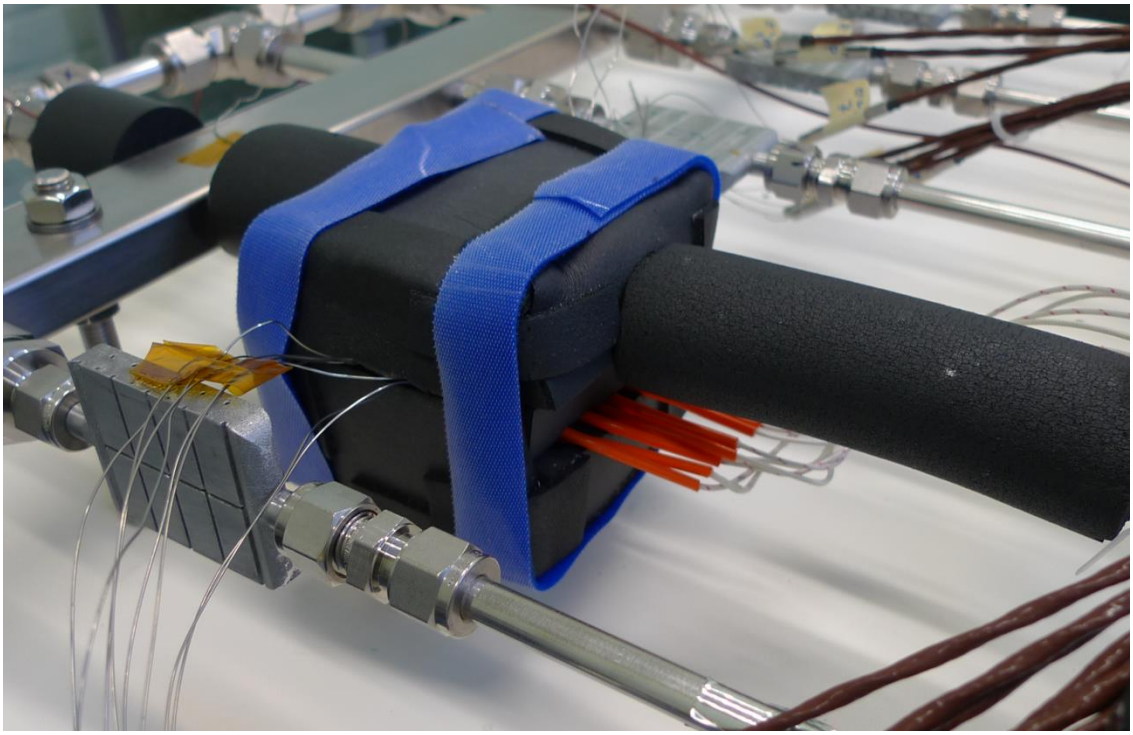

Figure 15 Photo of an evaporator after it is covered in insulation

V. Heat Transfer Coefficient calculation

The heat transfer coefficient between the fluid and the walls of the channel is usually calculated with:

$$h_{\text{fluid–wall}} = \frac{q_{\text{channel}}}{(T_{\text{wall}} - T_{\text{fluid}})}, \quad \textbf{(1)}$$

The temperature of the fluid T_{fluid} can be measured relatively simple. However, determining the temperature of the channel wall T_{wall} and the heat flux on the channel q_{channel} is not so straightforward when the heat flux is very high. This is illustrated with Figure 16, which shows a schematic drawing of the cross section of an evaporator. At the bottom of the evaporator is a heater, which generates a uniform heat flux $q_{\text{interface}}$. It is not possible to measure the temperature exactly at the wall. Instead, the temperature is measured with a sensor somewhere between the heater and the channel (see T_{sensor} in Figure 16). Assuming a uniform heat flux $q_{\text{interface}}$, the temperature at the bottom wall of a channel can be calculated with:

$$T_{\text{wall}} = T_{\text{sensor}} - \frac{q_{\text{interface}}}{k_{\text{alu}}} s \quad \textbf{(2)}$$

where $s_{s\text{-}w}$ is the distance between the sensor and the wall. In the test performed for this project, the heat flux at the interface is up to 50 W/cm^2. This is a relatively high heat flux which results in significant temperature gradients through the aluminium. For example, with a heat flux $q_{\text{interface}}$ of 50 W/cm^2 and an aluminium evaporator (k_{alu}=173 W/mK), the temperature gradient $q_{\text{interface}}$ /k_{alu} is 2.9°C/mm. Since the channel has a typical diameter of 0.6 mm, there can be a variation in the channel wall temperature of 1.74°C. This temperature variation results in a non-uniform heat flux around the channel wall (i.e. the heat flux at the bottom of the channel is higher than at the top). Because q_{channel} is not uniform, equation (1) is less suitable to calculate the HTC and compare the different evaporator samples.

In a typical evaporator, the channels are located as close to the interface as possible. A typical distance between the channels and interface is 0.3 mm. This distance is indicated as the 'virtual interface' with a dashed line in Figure 16. To compare the different evaporators, a heat transfer coefficient at this virtual interface is defined as:

$$h_{\text{virtual interface}} = \frac{q_{\text{interface}}}{(T_{\text{virtual interface}} - T_{\text{fluid}})}, \quad \textbf{(3)}$$

with

$$T_{\text{virtual interface}} = T_{\text{sensor}} - \frac{q_{\text{interface}}}{k_{\text{alu}}} s_{\text{vi}} \quad \textbf{(4)}$$

Where $s_{\text{s-vi}}$ is the distance between the sensors and the virtual interface. These equations are used to calculate the heat transfer coefficient between the fluid and the virtual interface in the next sections.

Besides the heat transfer coefficient between the fluid and the evaporator, there is also a heat transfer coefficient between the copper heater block and the aluminium evaporator. This heat transfer coefficient at the copper-aluminium interface is defined as:

$$h_{\text{copper-alu interface}} = \frac{q_{\text{interface}}}{(T_{\text{copperinterface}} - T_{\text{alu interface}})}, \quad \textbf{(5)}$$

With

$$T_{\text{copperinterface}} = T_{\text{sensorin copper}} - \frac{q_{\text{interface}}}{k_{\text{copper}}} s_{\text{s-copper}} \quad \text{and} \quad T_{\text{alu interface}} = T_{\text{sensorin alu}} + \frac{q_{\text{interface}}}{k_{\text{alu}}} s_{\text{s-alu}} \quad \textbf{(6)}$$

Where $s_{\text{s-copper}}$ and $s_{\text{s-alu}}$ are the distances between the temperature sensor and the interface in the copper and aluminium respectively.

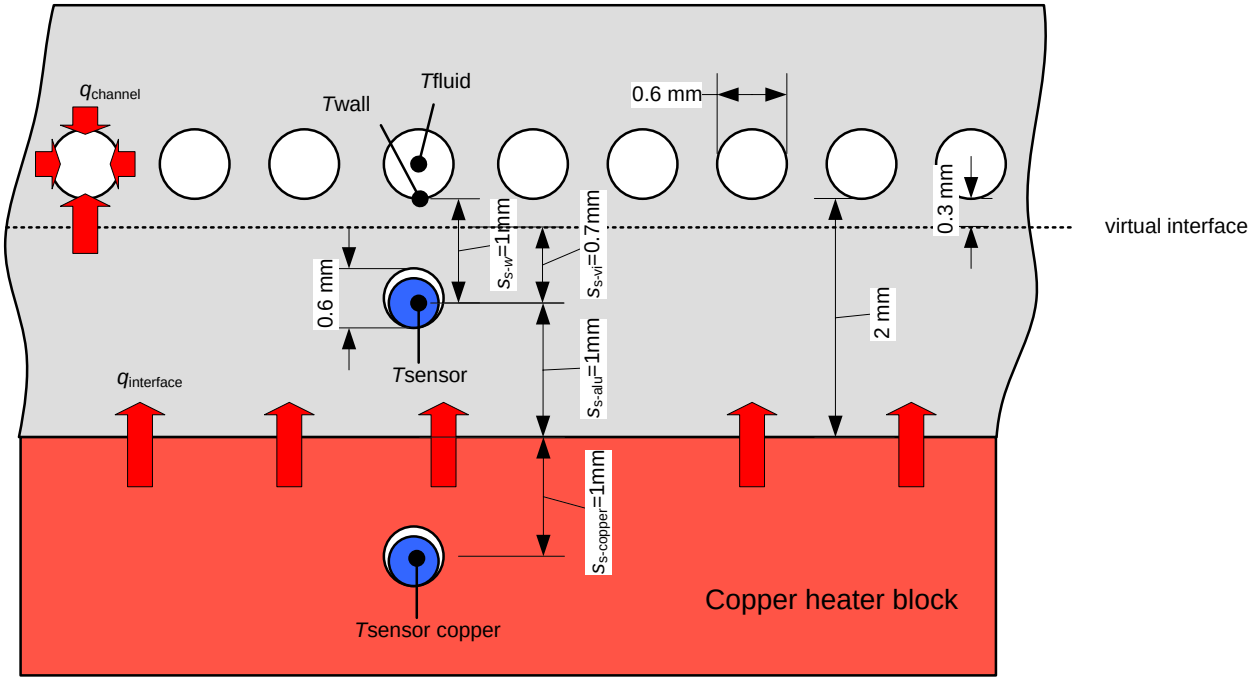

Figure 16 Schematic drawing of the copper heat block with aluminium evaporator

VI. Test results

A. Sample 1 in horizontal orientation

Figure 17 shows the heat input that is applied on evaporator sample 1 (straight channels) in horizontal orientation. The initial heat load is 722 W, which results in a heat flux on the evaporator surface of 50W/cm^2. After a certain time, the heat flux is reduced to 40, 30, 20, and 10W/cm^2. Figure 18 shows the fluid mass flow during the test. While the heat load is maintained at a constant value (e.g. at 722W), the mass flow is reduced in steps (e.g. from 25.9 g/s to 7.4 g/s). As a result, the vapour mass fraction at the exit of the evaporator increases, which can be seen in Figure 19. At a heat input of 722W and a vapour mass fraction of 0.2, the pressure drop is 0.47 bar (see Figure 20), which is close to the calculated value of 0.6 bar. When the mass flow and heat input decreases, the pressure drop also decreases. Figure 21 shows the measured temperatures in the evaporator and the saturation temperature at the inlet and outlet of the evaporator. The blue lines indicate the temperature sensors near the inlet of the evaporator and the red lines near the exit (see Figure 7 for the position of the temperature sensors). The sensors on the left side are indicated with solid lines, and on the right side with dashed lines. When the vapour mass fraction is increased to 0.7, the temperature near the exit of the evaporator (indicated with the red lines) becomes higher. This indicates that the heat transfer becomes less effective. With a heat input of 722W and a vapour mass fraction of 0.5 (10.4 g/s mass flow), the measured temperatures in the evaporator are between 103.5 and 106°C, i.e. a temperature difference of ~10°C between the fluid and the sensor. However, part of this temperature difference is because the heat flux has to travel through a 1 mm thick layer of aluminium between temperature sensors and the channels, which results in a 2.9°C temperature difference (see previous section). In a typical evaporator, the channels are located as close to the interface as possible. A typical distance between the channels and interface is 0.3 mm (see also Figure 16), which would result in only a 0.9 °C temperature difference. Hence, Figure 22 shows the temperatures at a 'virtual interface' which is located 0.3 mm below the channels. These temperatures are significantly lower. With a heat input of 722W and a vapour mass fraction of 0.5, no dry-out is observed and the evaporator temperature is well below the requirement of 110°C. Note that the outlet saturation temperature of the fluid is lower than the inlet saturation temperature. The reason for this is that the pressure at the evaporator outlet is lower than the inlet pressure, which results in a lower saturation temperature at the outlet (since pressure and saturation temperature are directly related for two-phase fluids).

Besides the temperature difference between the fluid and the evaporator, there is also a significant temperature difference between the copper heater block and the aluminium evaporator. This can be seen in Figure 23, which shows the average temperature of the 8 sensors in the copper block and in the evaporator.

Figure 24 shows the calculated heat transfer coefficients (see equation (3) and (5) in the previous section). The heat transfer coefficient between the fluid and evaporator is approximately 7 W/cm^{2}K with q=50W/cm^2 and x_{exit}=0.5. The heat transfer coefficient between the evaporator and copper heater block is approximately 9 W/cm^{2}K.

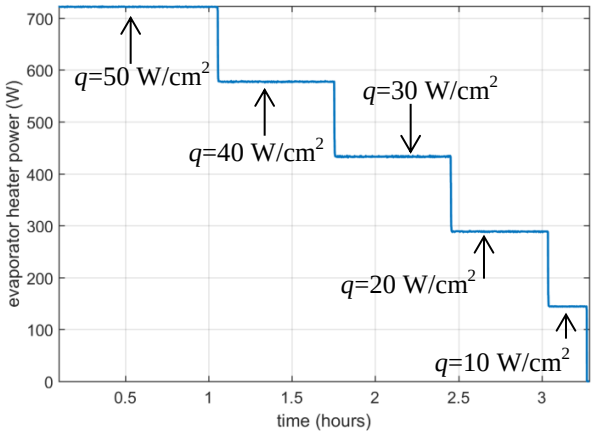

Figure 17 Evaporator power during the measurement

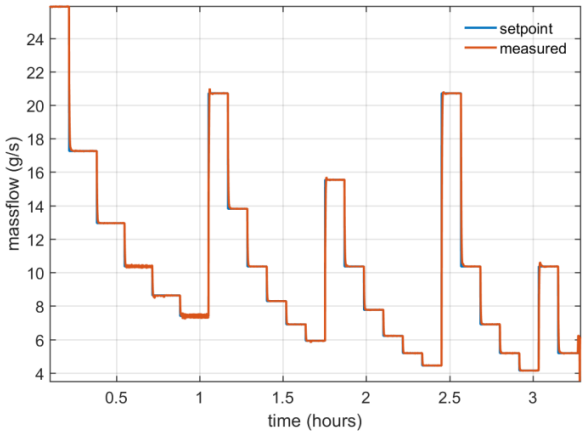

Figure 18 Mass flow during the measurement

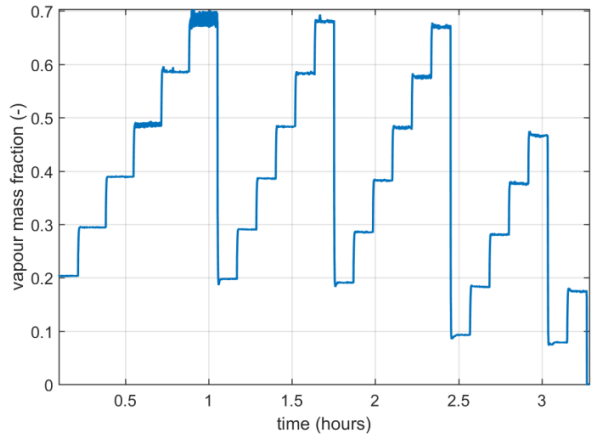

Figure 19 Vapour mass fraction at evaporator exit

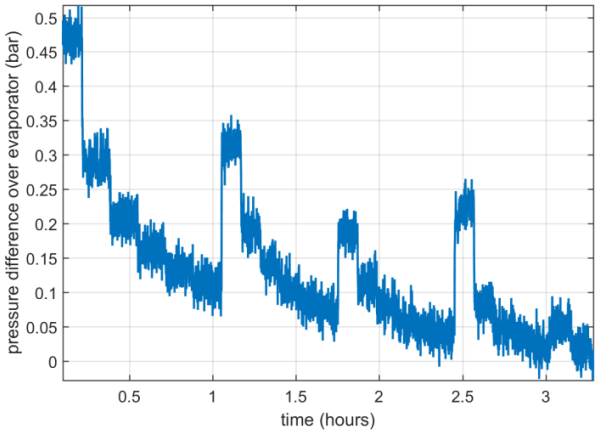

Figure 20 Pressure drop over evaporator

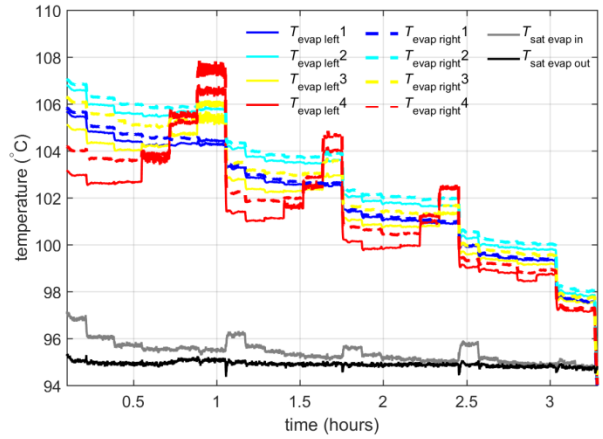

Figure 21 Temperatures in the evaporator

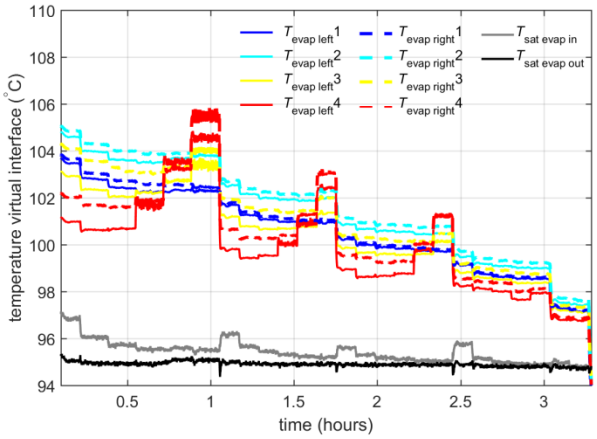

Figure 22 Calculated temperatures at the virtual interface of the evaporator

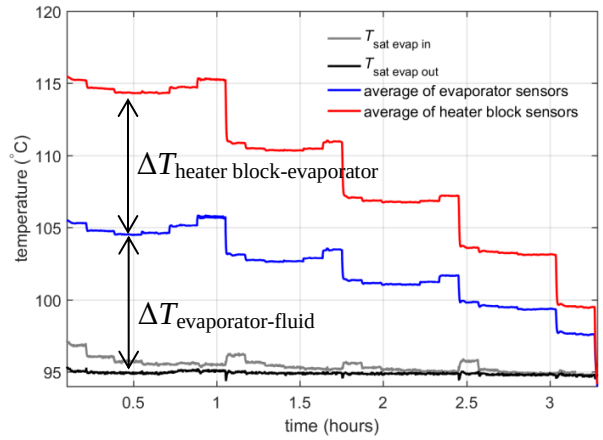

Figure 23 Evaporator and heater block temperatures

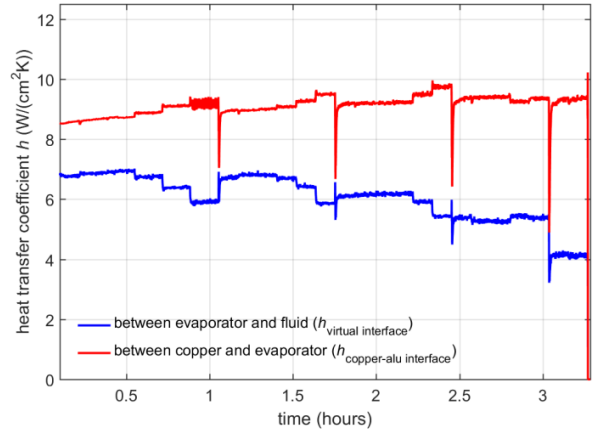

Figure 24 Calculated heat transfer coefficient

B. Sample 1 in vertical orientation

In the measurement described above, the evaporator is in a horizontal orientation. The evaporator has a manifold that distributes the fluid over the different parallel channels (see Figure 4). When the outlet and inlet manifold have a vertical orientation (i.e. when the evaporator is rotated with 90°), it could be that the fluid will not be evenly distributed over the channels because of gravity effects. This effect is especially important when the Froude number is low. This could result in overheating of one side of the evaporator. To test this, a measurement was carried out in which evaporator 1 was rotated with 90° (see Figure 14). Figure 25 shows the measured temperatures in the evaporator. The measured temperatures are very similar to the measured temperatures when the evaporator is in a horizontal orientation. It can therefore be concluded that the orientation does not have a significant influence on the thermal performance of the evaporator.

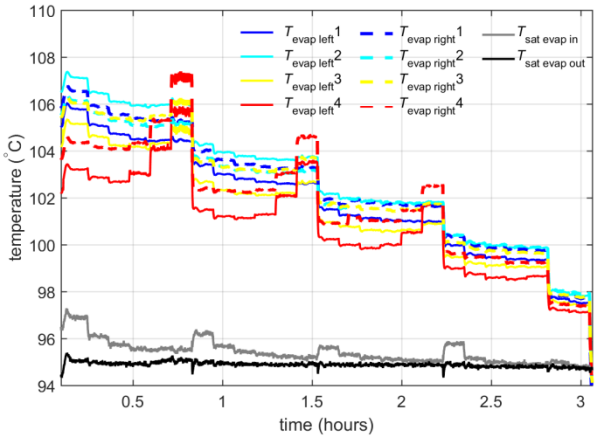

Figure 25 Measured temperatures with a tilted evaporator

C. Testing of other samples and summary of test results

Similar tests as described in the previous sections were carried out for all eight evaporator samples. Figure 26 shows the heat transfer coefficient between the evaporator and the fluid (calculated with equation (3)) for two different heat fluxes and Figure 27 shows the pressure difference. The figures show that sample 1, 2, 3, 7, and 8 are all feasible for the evaporator design, since for all these samples, the evaporator temperature is well below the requirement of 110°C. Sample 6 shows a very large difference between the measured temperatures on the left side and on the right side, and is therefore not useable. Samples 4 and 5 have a high pressure drop and are therefore less attractive.

Sample 1 (straight parallel channels) is the most simple and the pressure drop of this sample can be calculated most accurately. Sample 8 has a slightly higher heat transfer coefficient and a lower pressure drop, but due to the changes in channel diameter of this sample, the pressure drop cannot be accurately calculated with existing empirical correlations. For this reason, sample 1 is selected to be further developed in the detail design phase of the cooling system for the aircraft application. The heat transfer coefficient between evaporator sample 1 and the fluid is 6.8 W/(cm^{2}K) when the heat flux is 50 W/cm^2. This means that there will be a temperature gradient between the fluid and evaporator of 7.4°C. The heat transfer coefficient at the interface between the evaporator and the heat source is measured to be approximately 9 W/(cm^{2}K), which result in a temperature gradient over the evaporator/heater interface of 5.6°C. The total temperature gradient between the fluid and the heat source surface is then approximately 13°C when the heat flux is 50 W/cm^2.

Sample 1 and sample 8 were tested in a different orientation. The measured temperatures are very similar to the temperatures when the evaporator is in the horizontal orientation, which indicates that the orientation does not have a significant influence on the thermal performance of the evaporator.

Before the measurements were carried out, it was conservatively assumed that the vapour mass fraction x_{exit} should remain below 0.2 to prevent dry-out when the heat load is high. However, the measurements show that no dry-out occurs and a vapour mass fraction x_{exit} of 0.5 or 0.6 is sufficient. This means that the massflow can be three times lower than originally assumed.

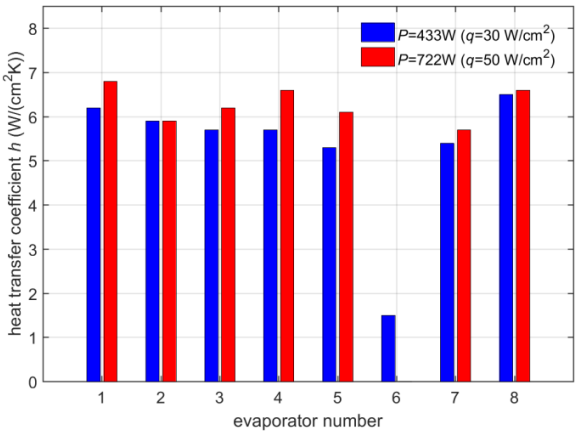

Figure 26 Heat transfer coefficient between the fluid and evaporator with a massflow of 10.4 g/s

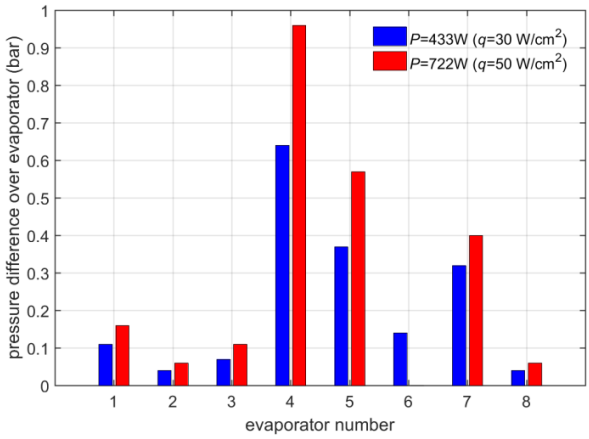

Figure 27 Pressure difference over the evaporator with a massflow of 10.4 g/s

VII. Conclusions

The tests show that several evaporator samples are suitable to cool a 722W heat load and a heat flux of 50W/cm^2. The sample with simple straight parallel channels is selected to be further developed in the detail design phase, although some other samples had a slightly better performance. The reason for this is that with existing empirical correlations, the pressure drop can only be calculated with reasonable accuracy for simple straight channels. At a heat flux of 50W/cm^2, there is a temperature gradient between the fluid and evaporator of 7.4°C, which is well below the requirement. The tests show that the 3D printed aluminium evaporators are able to keep the heat source well below its maximum temperature, and are therefore very suitable for cooling of electronic components that generate a high heat flux.

Appendix

Figure 28 to Figure 32 show cross sections of several evaporator samples.

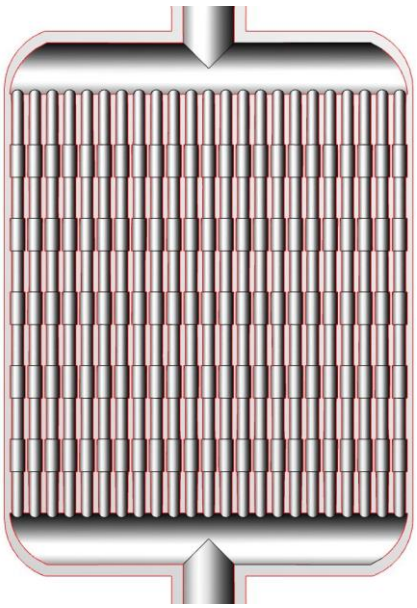

Figure 28 Evaporator sample 2

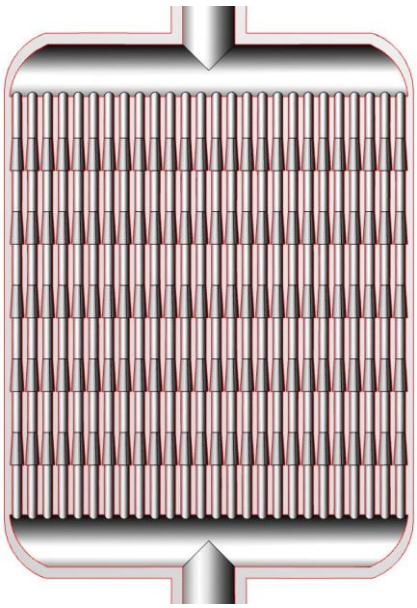

Figure 29 Evaporator sample 3

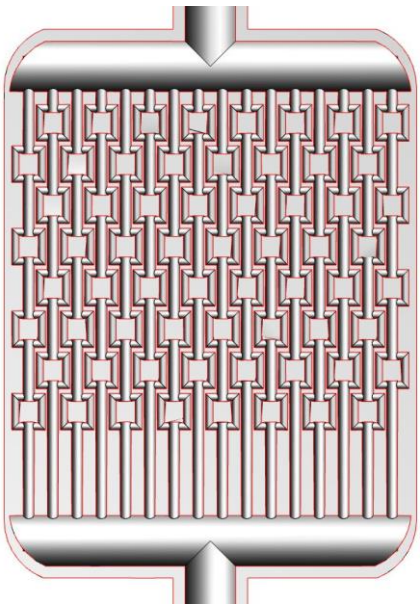

Figure 30 Evaporator sample 5

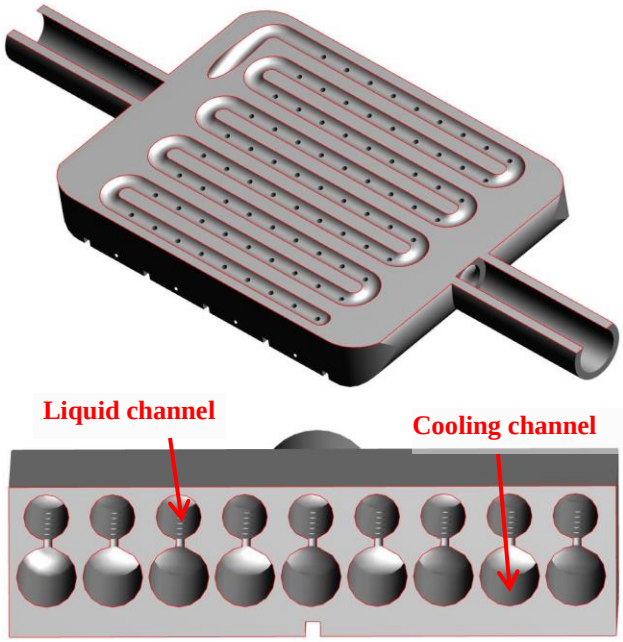

Figure 31 Evaporator sample 6

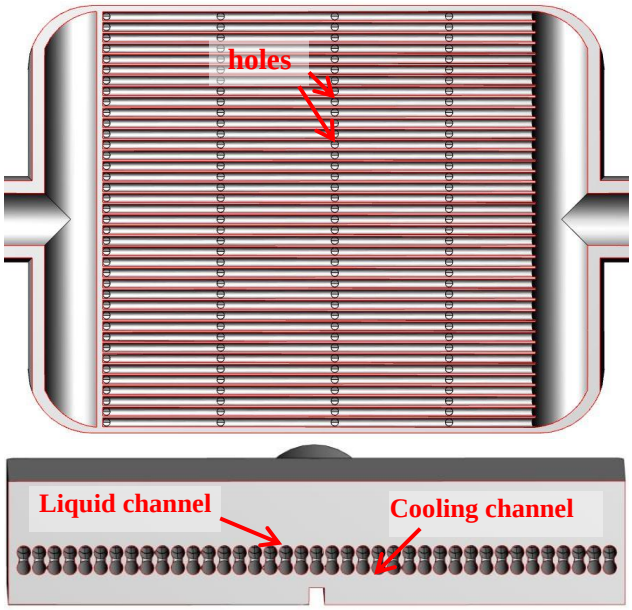

Figure 32 Evaporator sample 7

Acknowledgments

This project is carried out in cooperation with Thales Avionics Electrical Systems SAS. It has received funding from the Clean Sky 2 Joint Undertaking under the European Union's Horizon 2020 research and innovation program under grant agreement No 738094.

References

[1]Ebadian, M.A., Lin, C.X., "A Review of High-Heat-Flux Heat Removal Technologies", ASME. J. Heat Transfer. 2011; 133(11):

[2]van Gerner, H. J., Bolder, R., van Es, J., "Transient modelling of pumped two-phase cooling systems: Comparison between experiment and simulation with R134a", 47th International Conference on Environmental Systems, ICES-2017-037

[3]de Smit, M.,van Gerner, H. J., "Optimization of a Pumped Two Phases Cooling System using Additive Manufacturing", Direct Digital Manufacturing Conference 2018, DDMC-2018-1177

[4]van Gerner, H. J., Braaksma, N., "Transient modelling of pumped two-phase cooling systems: Comparison between experiment and simulation", 46th International Conference on Environmental Systems, ICES-2016-004

[5]Incropera, F.P., Dewitt, D.P., Bergman, T.L., Lavine, A.S., "Fundamentals of heat and mass transfer", (John Wiley & Sons, Hoboken, 2007)